ANGULAR DISTRIBUTIONS FOR (d,p) AND (d,t) REACTIONS ON ^{154}Sm, ^{166}Er, ^{170}Yb AND ^{176}Yb TARGET NUCLEI

By M. Jaskóła

Institute of Nuclear Research, Warsaw*

B. Elbek, K. Nybø and P. O. Tjøm

The Niels Bohr Institute, University of Copenhagen, Denmark

(Received May 6, 1978)

The angular distributions for the reactions ^{154}Sm(d,p), ^{166}Er(d,p), ^{170}Yb(d,p), ^{176}Yb(d,p) and ^{154}Sm(d,t), ^{166}Er(d,t) have been measured at a deuteron energy of 12.08 MeV. The reaction products were analysed in a magnetic spectrograph or by means of a solid state detector. The angular distributions for particle groups corresponding to 66 levels in the final nuclei have been analysed in terms of the DWBA method. On this basis the transferred angular momentum l was determined and the Nilsson Model assignments of the levels were determined or confirmed. Several of the angular distributions deviate considerably from the calculated shapes. Possible reasons for these deviations are discussed.

1. Introduction

The (d,p) and (d,t) reactions have been extensively used at the Niels Bohr Institute for studying the level structures of deformed nuclei. The results of these studies have been published in a number of papers [1–5] in which the assignments of specific quantum numbers were made mainly on the basis of absolute cross sections, intensity patterns for rotational bands and rudimentary angular distributions based on a few angles only. In several cases it was felt necessary to perform more complete angular distribution measurements. The results of such studies for six selected reactions are presented in this paper. The complete angular distributions have in several cases been decisive for the unambiguous assignment of quantum states. This is especially the case for the $l = 0$ angular momentum transfers [4, 6], the identification of which rests mainly on the angular distributions. The angular distributions themselves are also interesting and allow for a detailed comparison with the results of the distorted wave Born approximation (DWBA) calculations for a wide range of l values.

* Address: Instytut Badań Jądrowych, Hoża 69, 00-681 Warszawa, Poland.

2. Experimental procedures

The experimental procedures were for most of the distributions identical to those described earlier [7]. Deuterons with an energy of 12.08 MeV from the Niels Bohr Institute's EN tandem accelerator hit carbon backed targets prepared by evaporation of separated isotopes reduced to metals. The reaction products were analysed in a magnetic spectrograph with photographic plate detection. The spectra were recorded for each 5° in the range from 5° to 50° and for each 15° in the range from 60° to 150°. The exposure beam charges at each angle ranged from 3000 μC to 8000 μC.

The (d,p) angular distributions from Yb targets were determined by means of a Li-drifted Si solid state detector in a scattering chamber. In this way the angular distribution could be recorded somewhat faster than when a spectrograph was used, but at the expense of resolution. The angular range obtainable was 40° to 160° in 10° steps.

The absolute cross sections were in all cases determined by normalization to the cross section for elastic deuteron scattering plus the cross section for the inelastic scattering to the first rotational state in the target nucleus. This "quasi-elastic" cross section had earlier been determined in separate experiments.

3. Experimental results and discussion

The spectra for the different reactions have been published earlier (Yb, Ref. [1], Er, Ref. [3] and Sm, Ref. [7]). The absolute cross sections for the main groups are collected in Tables I to V and the angular distributions are represented in Figs 1 to 9 where the corresponding calculated distributions are also shown in terms of DWBA code DWUCK. The Nilsson assignments given for each level are partly based on the cross section patterns discussed in the references quoted above and partly on the shape of the angular distributions reported here.

The discussion given below mostly concerns the characteristic similarities or differences between distributions corresponding to the same l-value. The optical parameters used in the analysis are given in Table VI. The parameters used in the analysis of the (d,t) distributions are the same as those used earlier in the analysis of similar data for Gd targets [7] (set A) and those used in the coupled-channels calculation (set B) by Ascuitto et al. [14]. The parameters for the (d,p) distributions are average values of the parameters given in Ref. [5]. None of the parameters sets have been adjusted to give an optimum fit (on the average better agreement for the (d,t) angular distribution is obtained with set B of optical parameters). A slightly different set of deuteron parameters [9] gives an improved fit to elastic deuteron scattering, but introduced violent fluctuations in the calculated (d,t) distributions for even l-values which deviate from observation. Similar remarks apply to the (d,p) distributions of even l.

The experimental (d,t) distributions are in general quite similar to those published earlier for the Gd nuclei [7, 10].

In the present paper we show four examples of $l = 0$ (d,t) distributions. In ^{153}Sm the ground state Nilsson assignment for the 412 keV state is $\frac{1}{2}\frac{1}{2}+[400]$. This state is,

TABLE 1

Energy levels populated in the ^{154}Sm(d, t)^{153}Sm reaction

Peak no	Energy (keV)	Nilsson assignment	$d\sigma/d\Omega$ (μb/sr)															
			5°	10°	15°	20°	25°	30°	35°	40°	45°	50°	60°	75°	90°	105°	125°	150°
1	0	$\frac{3}{2}\frac{3}{2}+[651]$	—	13	30	50	86	102	115	126	160	180	215	165	145	91	60	40
2	34	$\frac{3}{2}\frac{3}{2}-[521]$	—	10	11	11	12	16	33	45	46	48	44	38	23	16	5	5
3	64	$\frac{9}{2}\frac{3}{2}+[651]$	—	—	2	6	14	40	72	102	140	150	152	152	103	81	37	36
4	94	$\frac{11}{2}\frac{11}{2}-[505]$	—	21	20	18	20	21	38	50	79	85	111	125	125	94	76	71
5	126	$\frac{3}{2}\frac{3}{2}-[532]$	—	47	51	46	50	63	91	113	135	122	126	91	59	35	20	14
6	171 180	$\frac{7}{2}\frac{3}{2}-[521]$ $\frac{5}{2}\frac{3}{2}-[532]$	—	4	—	15	33	60	84	95	111	124	134	136	92	70	37	29
7	194	$\frac{13}{2}\frac{3}{2}-[651]$	—	—	—	—	—	—	3	12	27	35	58	68	58	49	41	34
8	262	$\frac{7}{2}\frac{3}{2}-[532]$	—	3	9	—	34	64	85	101	130	139	174	183	127	108	61	51
9	320	$\frac{3}{2}\frac{3}{2}+[402]$	—	37	93	160	262	305	360	400	500	635	797	715	565	455	284	240
10	360	$\frac{5}{2}\frac{3}{2}+[402]$	—	3	10	13	32	25	32	42	52	56	67	56	41	29	17	14
11	402	$\frac{3}{2}\frac{1}{2}-[530]$	—	118	185	240	228	260	345	540	660	650	604	490	298	220	124	84
12	412	$\frac{1}{2}\frac{1}{2}+[400]$	730	570	335	188	298	510	785	940	1010	1010	950	970	676	498	299	220
13	480 492		—	3	9	15	19	26	27	28	38	51	66	64	71	51	56	37
14	523	$\frac{7}{2}\frac{1}{2}-[530]$	—	26	29	40	54	66	71	77	90	102	156	147	148	116	101	78
15	698	$\frac{1}{2}\frac{1}{2}-[521]$	—	7	10	8	13	13	17	22	29	31	30	24	17	12	8	5
16	732	$\frac{1}{2}\frac{1}{2}+[660]$	95	65	33	18	30	73	115	153	185	192	190	220	190	138	114	90
17	764 776 786		—	4	10	20	28	45	52	61	90	112	135	110	98	58	43	32
18	1532	$\frac{7}{2}\frac{7}{2}+[404]$	—	13	10	16	23	35	39	46	68	98	161	189	164	159	121	110
19	1558		—	—	—	2	5	10	10	12	16	17	26	29	20	17	13	13

TABLE II

Energy levels populated in the $^{166}Er(d,t)^{165}Er$ reaction

Peak no	Energy (keV)	Nilsson assignment	$d\sigma/d\Omega$ (μb/sr)														
			10°	15°	20°	25°	30°	35°	40°	45°	50°	60°	75°	90°	105°	125°	150°
1	0	$\frac{5}{2}\frac{5}{2}-$[523]	—	—	1	3	5	6	10	12	20	30	32	34	27	17	9
2	98	$\frac{9}{2}\frac{5}{2}+$[642[	—	—	—	1	3	13	17	29	37	53	70	71	62	37	25
3	176	$\frac{9}{2}\frac{5}{2}-$[523]	—	—	—	—	1	1	3	6	10	15	27	33	35	27	21
4	242	$\frac{3}{2}\frac{3}{2}-$[521]	6	9	14	21	31	46	68	81	102	159	164	233	136	124	70
5	297	$\frac{1}{2}\frac{1}{2}-$[521]	5	10	11	11	21	31	41	59	72	92	88	92	70	39	25
6	355	$\frac{3}{2}\frac{1}{2}-$[521]	—	—	1	1	2	3	5	7	6	12	11	9	7	5	1
7	372	$\frac{7}{2}\frac{3}{2}-$[521]	—	—	4	13	25	—	59	69	98	164	182	217	165	136	70
8	507	$\frac{1}{2}\frac{1}{2}+$[660]	46	5	4	6	19	40	65	79	89	114	140	168	106	102	68
9	534	$\frac{3}{2}\frac{3}{2}+$[402]	10	14	14	18	24	29	43	66	102	169	198	305	230	—	140
10	547	$\frac{11}{2}\frac{11}{2}-$[505]	3	5	2	4	4	3	6	6	10	17	35	57	14	36	35
11	746	$\frac{1}{2}\frac{1}{2}+$[400]	8	4	1	3	11	28	53	62	72	114	150	190	140	139	85
12	760		—	—	—	—	3	4	4	6	11	15	18	40	23	24	18
13	1039	$\frac{3}{2}\frac{1}{2}-$[530]	—	—	6	6	10	16	23	31	—	65	75	96	70	56	40

TABLE III

Energy levels populated in the $^{154}Sm(d,p)^{155}Sm$ reaction

Peak no	Energy (keV)	Nilsson assignment	$d\sigma/d\Omega$ (μb/sr)												
			20°	25°	30°	35°	40°	45°	50°	60°	75°	90°	105°	125°	150°
1	0	$\frac{3}{2}\frac{3}{2}-[521]$	305	242	180	215	254	233	254	206	89	79	33	28	13
2	128	$\frac{7}{2}\frac{3}{2}-[521]$	120	200	277	335	340	314	285	321	242	175	86	67	58
3	153	$\frac{9}{2}\frac{5}{2}+[642]$	—	—	—	43	55	49	55	59	27	51	11	14	8.5
4	358	$\frac{13}{2}\frac{5}{2}+[642]$	—	—	8	—	23	29	43	51	59	52	—	39	26
5	427	$\frac{5}{2}\frac{5}{2}-[523]$	—	27	41	44	50	60	44	32	20	19	14	8	6.6
6	499	$\frac{7}{2}\frac{5}{2}-[523]$	215	340	390	600	480	485	480	211	203	142	86	60	80
7	821	$\frac{1}{2}\frac{1}{2}-[521]$	640	660	510	700	810	800	640	512	382	253	137	73	52
8	868	$\frac{3}{2}\frac{1}{2}-[521]$	29	26	—	40	74	71	71	50	27	29	17	12	7
9	908	$\frac{7}{2}\frac{5}{2}-[512]$	256	285	363	412	425	358	290	303	250	140	91	59	42
10	930	$\frac{5}{2}\frac{1}{2}-[521]$	180	268	173	330	295	430	310	186	155	88	58	31	23
11	962	$\frac{7}{2}\frac{5}{2}-[512]$	72	74	157	248	295	245	264	211	173	122	72	57	41
12	1080	$\frac{1}{2}\frac{1}{2}-[521]$	—	60	75	107	116	125	112	116	95	51	52	40	39

TABLE IV

Energy levels populated in the $^{166}Er(d,p)^{167}Er$ reaction

Peak no	Energy (keV)	Nilsson assignment	$d\sigma/d\Omega$ (μb/sr)											
			25°	30°	35°	40°	45°	50°	60°	75°	90°	105°	125°	150°
1	79	$\frac{9}{2}\frac{7}{2}+[633]$	—	10	13	20	19	23	19	20	9	9.5	8	5.3
2	208	$\frac{1}{2}\frac{1}{2}-[521]$	235	315	300	385	343	338	292	198	149	70	51	21
3	280	$\frac{5}{2}\frac{1}{2}-[521]$	33	53	66	70	67	64	63	48	38	26	18	16
4	295	$1\frac{3}{2}\frac{7}{2}+[633]$	6	—	8	11.5	16	22	27	30	42	31	34	25
5	347	$\frac{5}{2}\frac{5}{2}-[512]$	5	9	11	9.4	10.8	12	13	6.4	—	2.5	3	—
6	413	$\frac{7}{2}\frac{1}{2}-[521]$	51	100	114	134	131	143	125	111	84	60	37	24
7	430	$\frac{7}{2}\frac{5}{2}-[512]$	84	220	286	327	188	320	304	250	260	150	112	60
8	750	$\frac{3}{2}\frac{3}{2}-[521]$	43	40	44	53	44	42	42	22	34	14	11	5
9	802	$\frac{3}{2}\frac{1}{2}-[510]$	235	238	320	380	385	335	255	190	136	70	67	25
10	854	$\frac{5}{2}\frac{1}{2}-[510]$	49	62	82	77	82	76	73	62	80	25	33	6
11	894	$\frac{7}{2}\frac{3}{2}-[521]$	27	60	70	78	71	67	70	61	53	31	23	13.6
12	941	$\frac{7}{2}\frac{1}{2}-[510]$	13	10	39	13	23	22	20	22	27	9	13	—
13	1084	$\frac{3}{2}\frac{3}{2}+[402]$	—	30	35	—	25	38	21	14	15	—	9	10
14	1132	$\frac{1}{2}\frac{1}{2}+[400]$	210	143	167	148	96	90	73	64	39	31	18	12
15	1172		105	150	134	200	130	171	84	70	77	75	36	34
16	1384	$\frac{3}{2}\frac{3}{2}-[512]$	—	91	77	97	100	114	123	78	67	37	28	19
17	1440	$\frac{5}{2}\frac{3}{2}-[512]$	15	88	109	155	148	150	156	127	121	84	65	33

TABLE V

Energy levels populated in the $^{170}Yb(d,p)^{171}Yb$ and $^{176}Yb(d,p)^{177}Yb$ reactions

$^{170}Yb(d,p)^{171}Yb$

Peak no	Energy (keV)	Nilsson assigment	$d\sigma/d\Omega$ (μb/sr)												
			40°	50°	60°	70°	80°	90°	100°	110°	120°	130°	140°	150°	160°
1	0	$\frac{1}{2}\frac{1}{2}-[521]$ $\frac{3}{2}\frac{1}{2}-[521]$	—	130	145	140	100	78	86	66	44	36	30	21	16
2	72	$\frac{5}{2}\frac{1}{2}-[521]$	—	37	45	39	40	30	27	25	21	19	16	11	10
3	369	$1\frac{3}{2}\frac{7}{2}+[633]$	—	9	14	15	16	17	19	21	23	16	17	15	15
4	838	$\frac{7}{2}\frac{7}{2}-[514]$	—	80	49	40	38	40	32	27	24	23	15	16	15
5	995	$\frac{3}{2}\frac{1}{2}-[510]$	—	350	300	280	230	195	190	145	130	96	80	70	67

$^{176}Yb(d,p)^{177}Yb$

1	379	$\frac{3}{2}\frac{1}{2}-[510]$	940	660	480	540	450	305	205	158	126	105	88	64	63
2	424	$\frac{5}{2}\frac{1}{2}-[510]$	220	240	208	250	170	148	128	87	71	55	51	48	41
3	530	$\frac{7}{2}\frac{1}{2}-[510]$	70	73	115	80	76	59	47	44	31	32	24	25	25
4	615	$\frac{9}{2}\frac{1}{2}-[510]$	—	—	—	—	17	14	12	9	9	7	7	6	6
5	708	$\frac{3}{2}\frac{3}{2}-[512]$	248	232	285	245	176	168	130	86	75	64	45	38	45
6	774	$\frac{5}{2}\frac{3}{2}-[512]$	305	193	310	308	248	218	168	138	110	92	78	66	60
7	867	$\frac{7}{2}\frac{3}{2}-[512]$	170	155	154	175	128	112	92	82	54	48	41	42	32
8	1222	$\frac{7}{2}\frac{7}{2}-[503]$	450	400	385	415	365	346	280	200	184	150	132	118	102
9	1362	$\frac{3}{2}\frac{3}{2}-[501]$	—	1480	1620	1360	910	740	565	420	325	255	220	205	185
10	1447	$\frac{5}{2}\frac{3}{2}-[501]$	—	240	202	230	190	172	130	115	93	77	62	58	51
11	1496	—	—	178	142	120	75	70	59	45	36	34	31	22	25
12	1660	—	—	—	94	62	67	55	58	40	34	32	31	30	26
13	1920	—	—	—	510	550	370	360	270	170	135	123	115	95	76
14	2000	—	—	205	—	320	210	178	155	90	80	64	51	50	36

TABLE VI

Optical model parameters

		V (MeV)	M (MeV)	r_0 (fm)	a (fm)	r_0' (fm)	a' (fm)	r_c (fm)	calc.
	Deuterons	104	17	1.15	0.81	1.34	0.68	1.25	(d,p)
	Protons	54	17	1.25	0.65	1.25	0.47	1.25	
A	Deuterons	86	12	1.15	0.87	1.37	0.70	1.25	(d,t)
A	Tritons	154	12	1.10	0.75	1.40	0.65	1.25	
B	Deuterons	90.0	19.0	1.15	0.97	1.32	0.68	1.267	(d,t)
B	Tritons	171.0	12.0	1.16	0.75	1.50	0.82	1.267	

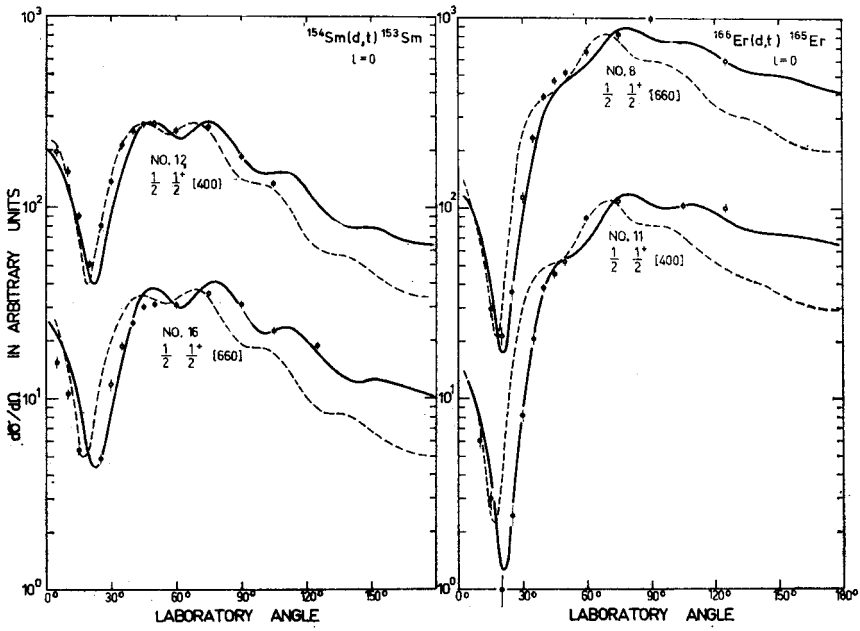

Fig. 1. Angular distributions for triton groups with $l = 0$ for the ^{154}Sm(d,t)^{153}Sm and ^{166}Er(d,t)^{165}Er reactions. The solid line shows the result of a DWBA calculation with the optical model parameters listed in Table VI (set A), the dashed line shows the results of a DWBA calculation with the parameters listed in Table VI (set B)

however, strongly $\Delta N = 2$ coupled to the $\frac{1}{2}\frac{1}{2}+[660]$ state which has a low cross section in itself, but which due to coupling derives considerable strength from the $\frac{1}{2}\frac{1}{2}+[400]$ state. The $\frac{1}{2}\frac{1}{2}+[660]$ state is found at 732 keV in ^{153}Sm and has an intensity corresponding to approximately 30% of the $\frac{1}{2}\frac{1}{2}+[400]$ state. The distributions for both states show a typical $l = 0$ behaviour at forward angles (cf. Fig. 1). Although both levels get their strength from the same quantum state, the angular distributions are somewhat different

at large angles where the $\frac{1}{2}\frac{1}{2}+[660]$ state reveals excess of intensity. The reason for this is unexplained.

Splitting of intensity between the same two state can be observed in ^{165}Er. The forward peak of the $l = 0$ distribution is less pronounced there and the minimum at ca 20° is very deep. These changes with respect to the ^{153}Sm case are well reproduced by the calculations. In ^{165}Er the observed distributions for the two components of the $\frac{1}{2}\frac{1}{2}+[400]$ state are almost identical.

There are several states populated in the (d,t) reaction by an $l = 1$ transfer, the corresponding distributions are shown in Fig. 2. In almost all cases the observed intensity at large angles is considerably less than that calculated by means of set A of the optical

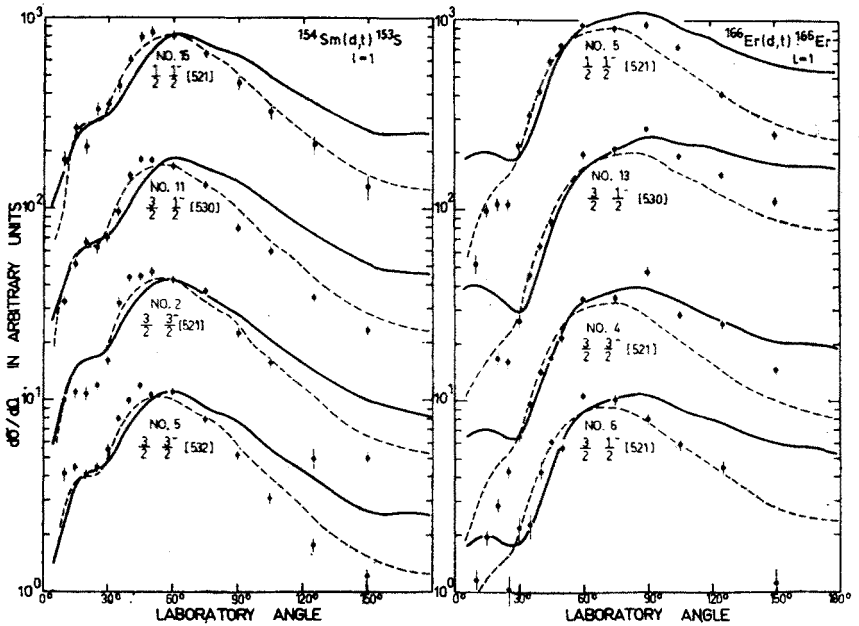

Fig. 2. Angular distributions for the triton groups with $l = 1$ for the ^{154}Sm(d,t)^{153}Sm and ^{166}Er(d,t)^{165}Er reactions

parameters. The shape of the $l = 1$ distributions are better reproduced by set B of these parameters. In the two Gd cases [7, 10] studied earlier it was found that for odd l the $= l+\frac{1}{2}$ distributions had larger intensity than the $j = l-\frac{1}{2}$ distributions at backward angles. The same effect can be observed although not very clearly in the data reported here.

The $l = 2$ distributions (Fig. 3) for ^{153}Sm show an example of $\Delta N = 2$ coupling similar to the one discussed for $l = 0$. The ground state in ^{153}Sm is $\frac{3}{2}\frac{3}{2}+[651]$ but with a 25% intensity admixture of the $\frac{3}{2}\frac{3}{2}+[402]$ state observed at 320 keV. The two distributions are similar at forward angles, but at large angles the $N = 6$ state has a relatively lower intensity. The $\frac{5}{2}\frac{3}{2}+[402]$ $l = 2$ distribution also observed in ^{153}Sm has at backward angles

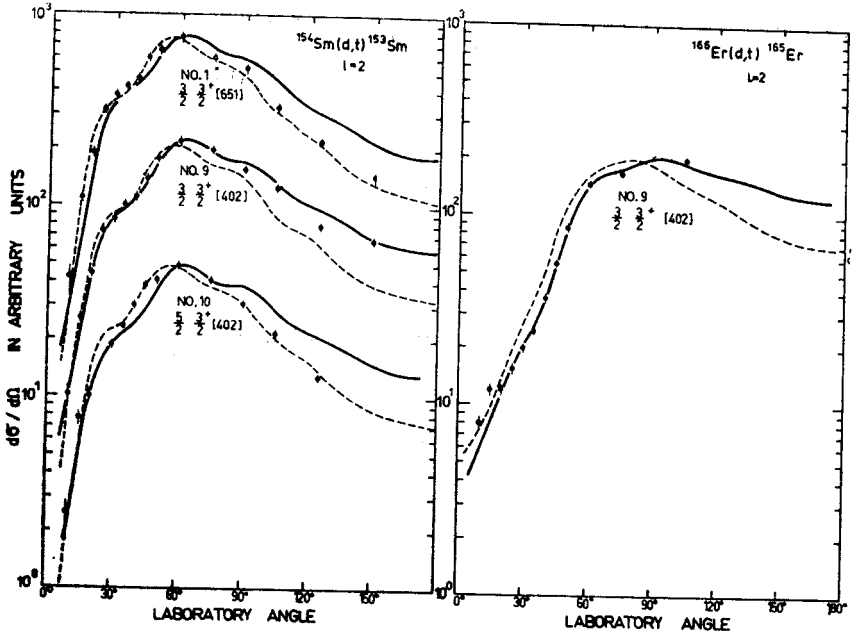

Fig. 3. Angular distributions for the triton groups with $l = 2$ for the ^{154}Sm(d,t)^{153}Sm and ^{166}Er(d,t)^{165}Er reactions

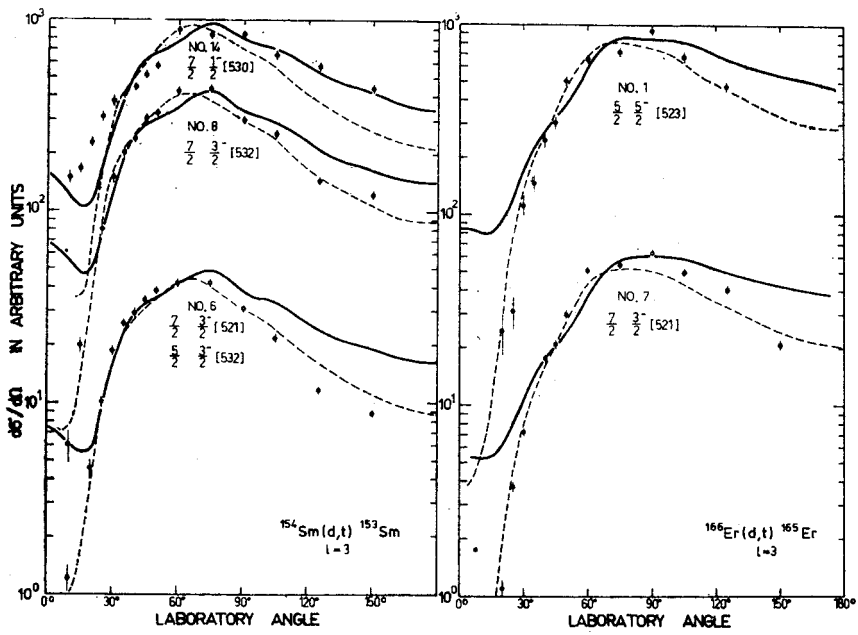

Fig. 4. Angular distributions for the triton groups with $l = 3$ for the ^{154}Sm(d,t)^{153}Sm and ^{166}Er(d,t)^{165}Er reactions

a lower intensity than the $\frac{3}{2}\frac{3}{2}+[402]$ distributions. This is in agreement with the general j-dependence observed [7] for even l. Finally, in ^{165}Er only the $l = 2$ distribution for the $\frac{3}{2}\frac{3}{2}+[402]$ state has been recorded. The maximum has been displaced with regard to the same distribution in ^{153}Sm by ca 40° towards larger angles. This displacement is well reproduced by the DWBA calculations.

The $l = 3$ (d,t) distributions are shown in Fig. 4. Here the DWBA calculations performed using set B of the optical parameters gives better agreement at small and at back angles. The first maximum at $\theta_{lab} = 40°$ to 50° is reproduced by both sets of optical parameters.

The $l = 4$ distributions shown in Fig. 5 reveal at small angles deviations between experiment and theory. The $\frac{7}{2}\frac{7}{2}+[404]$ distribution corresponds to $j = l-\frac{1}{2}$. In accordance with earlier observations [7] it is at large angles in much batter agreement with the calculated

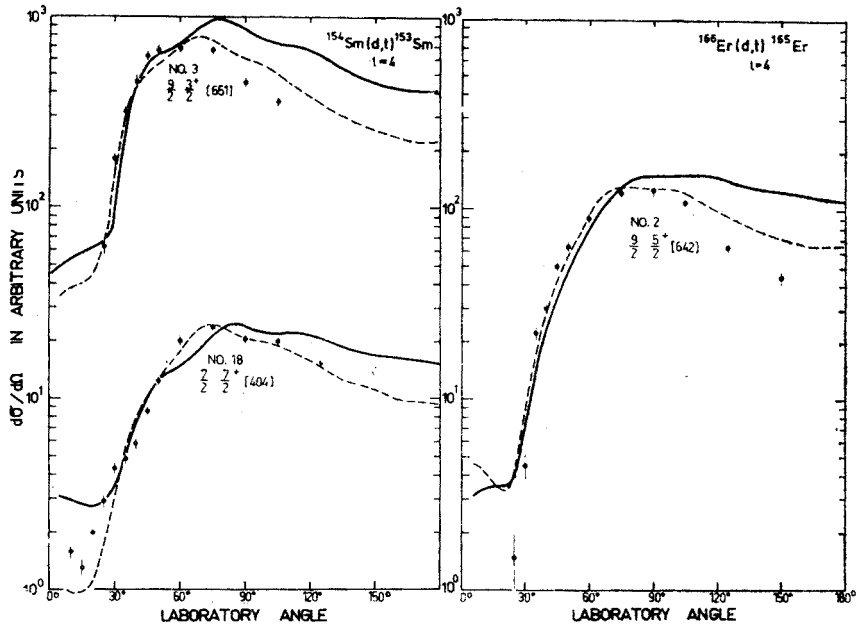

Fig. 5. Angular distributions for the triton groups with $l = 4$ for the ^{154}Sm(d,t) ^{153}Sm and ^{166}Er(d,t) ^{165}Er reactions

distributions than the distributions observed for the $\frac{9}{2}\frac{3}{2}+[651]$ and $\frac{9}{2}\frac{5}{2}+[642]$ states which correspond to $j = l+\frac{1}{2}$.

The $l = 5$ distributions presented in Fig. 6 show, in contrast to the $l = 3$ and 4 distribution discussed above some intensity at forward, angles for the two $\frac{11}{2}\frac{11}{2}-[505]$ distributions[1].

---

[1] Note: the $\frac{11}{2}\frac{11}{2}-[505]$ state in ^{165}Er is in Ref. [3] erroneously placed at 591 keV. The correct assignment is to the state at 547 keV.

On the other hand, the $l = 5$ distribution for the unambiguously assigned [3] $\frac{9}{2}\frac{5}{2}-$[523] state in ^{165}Er does not show any such intensity. Again there is no explanation for this rather considerable difference. It should be noted that the $\frac{1}{2}\frac{1}{2}-$[505] state is very weakly affected by couplings to other states and thus is a very pure state. In contrast the $\frac{9}{2}\frac{5}{2}-$[523] state is coupled to the $\frac{9}{2}\frac{3}{2}-$[521] one.

Only one pure $l = 6$ distribution, i.e. that of the well established [11] $\frac{1}{2}\frac{3}{2}+$[651] state in ^{153}Sm, could be recorded (see Fig. 6). There is a very low intensity at forward angles, again in contrast to the calculations which has been predicted by set A of optical

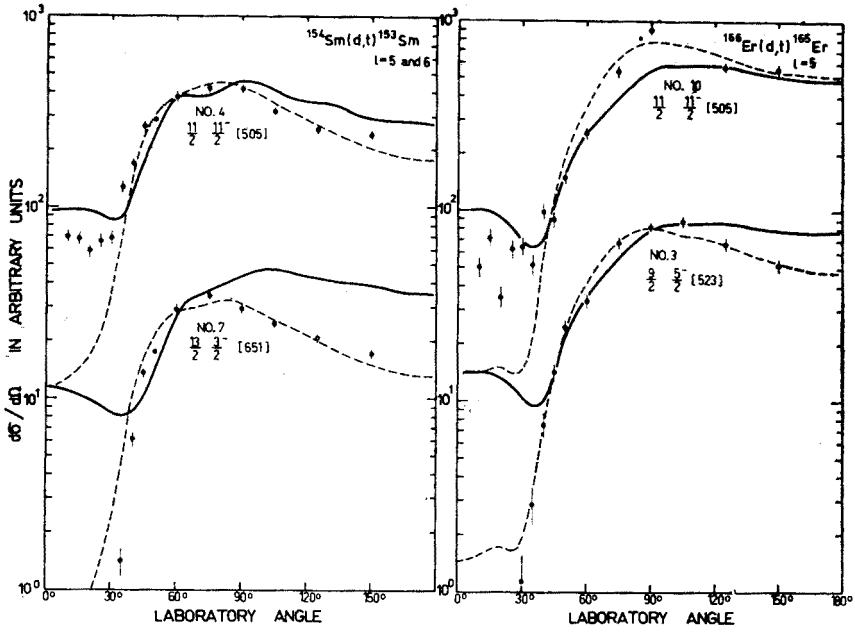

Fig. 6. Angular distributions for the triton groups with $l = 5$ and $l = 6$ for the ^{154}Sm(d,t) ^{153}Sm reaction, and with $l = 5$ for the ^{166}Er(d,t) ^{165}Er reaction

parameters. Also at back angles there are considerable deviations. However, the $l = 6$ character is evident from the position of the intensity maximum. Set B of optical parameters gives quite good agreement with the experimental distribution.

Only few examples of (d,p) angular distributions induced by $E_d = 12$ MeV for deformed nuclei [12, 13] have so far been recorded in the literature. It is therefore of some interest to examine the data obtained here for the Sm(d, p), Er(d, p) and Yb(d, p) reactions. Unfortunately, all the distributions correspond to $l = 1$ and $l = 3$ as no $l = 5$ distribution has sufficient intensity. All distributions are without discernible structure. The difference between $l = 1$ and $l = 3$ lies mostly in the slope of the curves at large angles. The theory predicts some characteristic differences at forward angles, but this region is experimentally not easily accessible because of severe background problems associated with the elastic scattering of deuterons. There has earlier [8] been uncertainty as to the

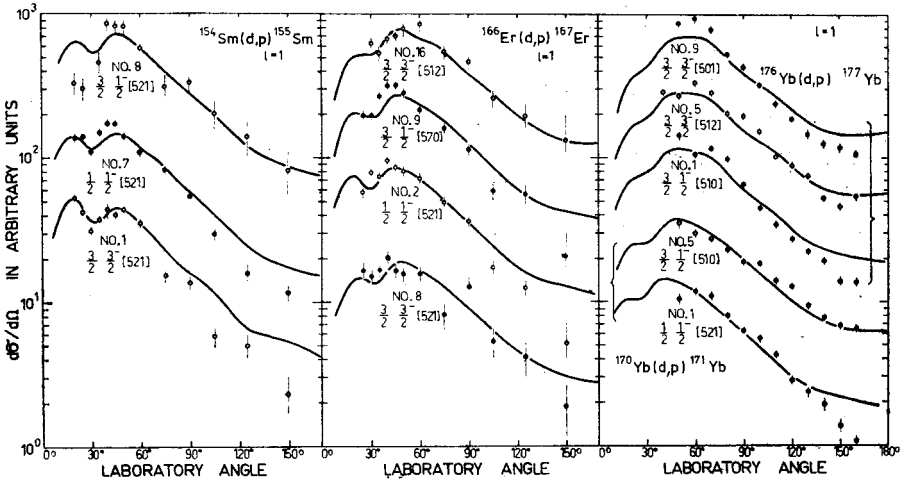

Fig. 7. Angular distributions for the proton groups with $l = 1$ for the ^{154}Sm(d,p) ^{155}Sm, ^{166}Er(d,p) ^{167}Er, ^{170}Yb(d,p) ^{171}Yb and ^{176}Yb(d,p) ^{177}Yb reactions

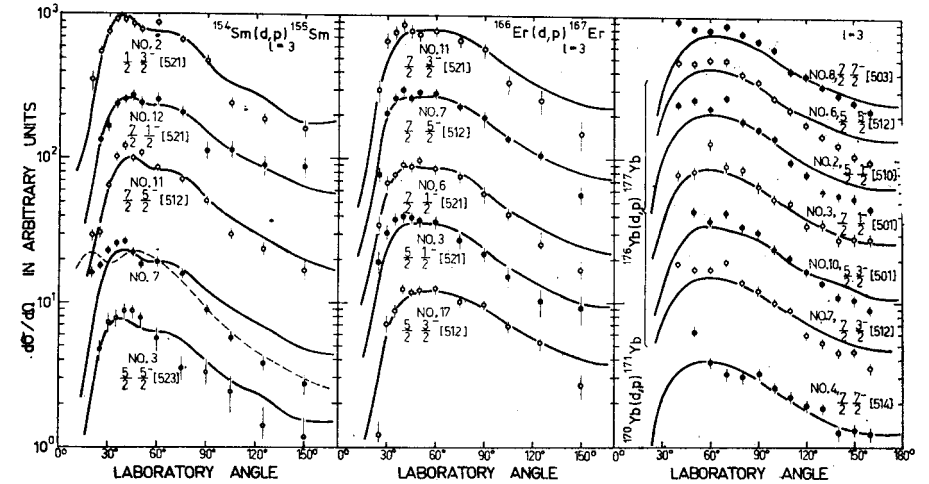

Fig. 8. Angular distributions for the proton groups with $l = 3$ for the ^{154}Sm(d,p) ^{155}Sm, ^{166}Er(d,p) ^{167}Er, ^{170}Yb(d,p) ^{171}Yb and ^{176}Yb(d,p) ^{177}Yb reactions

position of the $\frac{7}{2}\frac{5}{2}-[512]$ state in ^{155}Sm which could be either at 908 or at 962 keV. The distributions for the levels no 9 (908 keV) and 11 (962 keV) shown in Fig. 8 indicate that only level no 11 has a $l = 3$ distribution and that 962 keV is thus the preferred position for the $\frac{7}{2}\frac{5}{2}-[512]$ state.

The distributions given in Fig. 9 are the first examples of distributions for an even l-value known up to now. As it is seen in Fig. 9 the calculated shapes for $l = 0$ show strong oscillations which, however, are not very obvious in the experimental data. The calculated

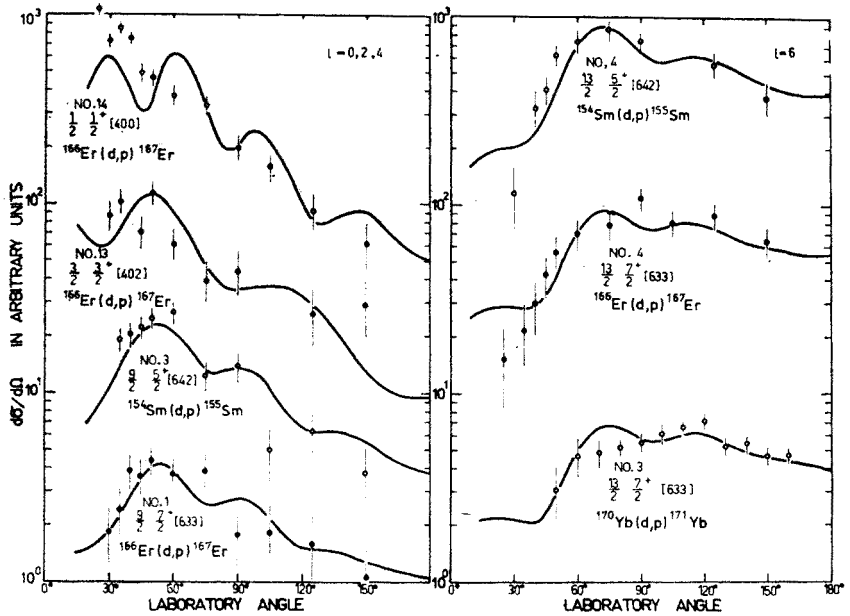

Fig. 9. Angular distributions for the proton groups with $l = 0$, $l = 2$ and $l = 4$ for the ^{154}Sm(d, p) ^{155}Sm and ^{166}Er(d,p) ^{167}Er reactions and with $l = 6$ for the ^{154}Sm(d,p) ^{155}Sm, ^{166}Er(d,p) ^{167}Er and ^{170}Yb(d,p) ^{171}Yb reactions

distribution for higher l-values follows more or less the data which are, however, partly of low accuracy because of insufficient intensity. The best data are for the three $l = 6$ distributions which are in fairly good agreement with the calculated curves.

4. *Conclusions*

From the data presented above it is clear that the general situation relative to the calculation of angular distributions for transfer reactions in deformed nuclei is not very satisfactory. At present, with an increasing amount of experimental data becoming available, it might be justified to attempt a more detailed theoretical analysis taking into account the coupling of channels and spin-orbit effects.

The CCBA (coupled-channels Born approximation) performed by Ascuitto and Sørensen for the ^{156}Gd(d,t)^{155}Gd reaction [10] for the $\frac{3}{2}-$, $\frac{5}{2}-$ and $\frac{7}{2}-$ members of the $\frac{1}{2}-$[530] band are shown in Fig. 10. It is evident that the CCBA calculations improve the agreement with experimental data.

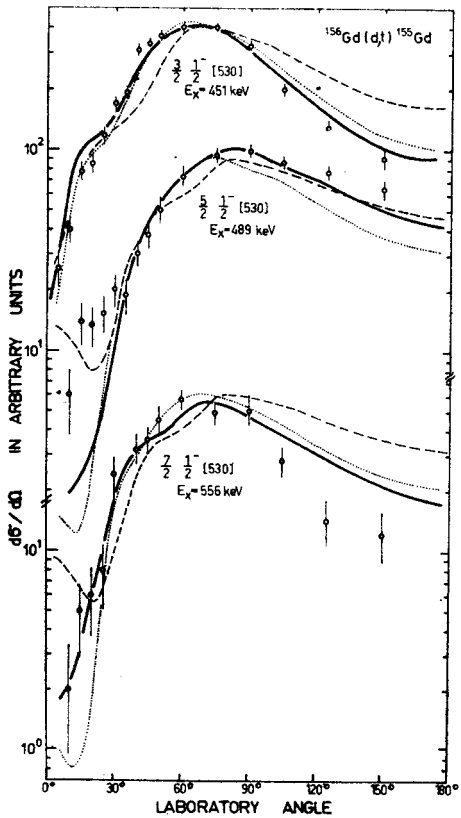

Fig. 10. Differential cross section for the ^{156}Gd(d,t) ^{155}Gd reaction leading to $\frac{3}{2}-$ (451 keV), $\frac{5}{2}-$ (489 keV) and $\frac{7}{2}-$ (556 keV) members of the $\frac{1}{2}-$[530] band of ^{155}Gd. The solid line represents the CCBA calculation with the parameters listed in Table VI (set B), whereas the dashed and dotted lines represent the DWBA calculation using the optical model parameters listed in Table VI (set A and B), respectively. The experimental data have been taken from Ref. [10]

The present work is the result of collaboration between the Niels Bohr Institute, Tandem Accelerator Laboratory, Risø and the Institute of Nuclear Research, Warsaw. One of the authors (M.J) wishes to thank the NBI authorities for their hospitality.

REFERENCES

[1] D. G. Burke, B. Zeidman, B. Elbek, B. Herskind, M. Olesen, *Mat. Fys. Medd. Dan. Vid. Selsk.* **35**, no. 2 (1966).
[2] P. O. Tjøm, B. Elbek, *Mat. Fys. Medd. Dan. Vid. Selsk.* **36**, no 8 (1967).
[3] P. O. Tjøm, B. Elbek, *Mat. Fys. Medd. Dan. Vid. Selsk.* **37**, no. 7 (1969).

[4] I. Kanestrøm, P. O. Tjøm, *Nucl. Phys.* **A179**, 305 (1972).
[5] B. Elbek, P. O. Tjøm, *Advances in Nuclear Physics*, vol. 3, ed. M. Baranger and E. Vogt, Plenum Press, New York 1969.
[6] I. Kansetrøm, P. O. Tjøm, J. Bang, *Nucl. Phys.* **A164**, 664 (1970).
[7] M. Jaskóła, K. Nybø, P. O. Tjøm, B. Elbek, *Nucl. Phys.* **A96**, 52 (1967).
[8] P. O. Tjøm, Thesis at University of Oslo, 1969.
[9] P. R. Christensen, A. Berinde, I. Neamu, N. Scintoi, *Nucl. Phys.* **A129**, 337 (1969).
[10] M. Jaskóła, P. O. Tjøm, B. Elbek, *Nucl. Phys.* **A133**, 65 (1969).
[11] G. Løvhøiden, P. O. Tjøm, L. Edvardson, *Nucl. Phys.* **A194**, 463 (1972).
[12] M. N. Vergnes, R. K. Sheline, *Phys. Rev.* **132**, 1736 (1963).
[13] R. H. Siemssen, J. R. Erskine, *Phys. Rev.* **146**, 911 (1966).
[14] R. J. Ascuitto, C. H. King, L. J. McVay, B. Sørensen, *Nucl. Phys.* **A226**, 453 (1974).